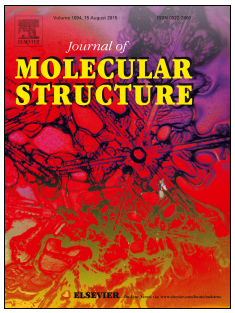

Design, synthesis and computational studies of *N*-(substituted-phenyl)-4-(4-phenyl-1-piperazinyl)butanamides as a potent anti-melanogenic and tyrosinase inhibitors

Hussain Raza, Muhammad Athar Abbasi, Aziz-ur Rehman, Sabahat Zahra Siddiqui, Mubashir Hassan, Syed Adnan Ali Shah, Muhammad Shahid, Hansol Hong, Sung-Yum Seo

PII: S0022-2860(20)30294-5

DOI: https://doi.org/10.1016/j.molstruc.2020.127969

Reference: MOLSTR 127969

To appear in: *Journal of Molecular Structure*

Received Date: 28 November 2019

Revised Date: 12 February 2020

Accepted Date: 24 February 2020

Please cite this article as: H. Raza, M.A. Abbasi, A.-u. Rehman, S.Z. Siddiqui, M. Hassan, S.A.A. Shah, M. Shahid, H. Hong, S.-Y. Seo, Design, synthesis and computational studies of *N*-(substituted-phenyl)-4-(4-phenyl-1-piperazinyl)butanamides as a potent anti-melanogenic and tyrosinase inhibitors, *Journal of Molecular Structure* (2020), doi: https://doi.org/10.1016/j.molstruc.2020.127969.

Credit Author Statment

Hussain Raza: Performed *in vitro* and *in vivo* experiments and wrote the initial draft of manuscript. **Sabahat Zahra Siddiqui** and **Aziz-ur-Rehman:** Synthesized the chemical compounds. **Mubashir Hassan:** Performed the *in silico* computational experiments. **Syed Adnan Ali Shah:** Done spectral analysis and characterization of compounds. **Muhammad Shahid:** Performed cytotoxicity experiments. **Hansol Hong:** Helped in the analysis of data. **Muhammad Athar Abbasi** and **Sung-Yum Seo:** Facilitated and supervised the whole study. Also checked and approved the final draft of this manuscript.

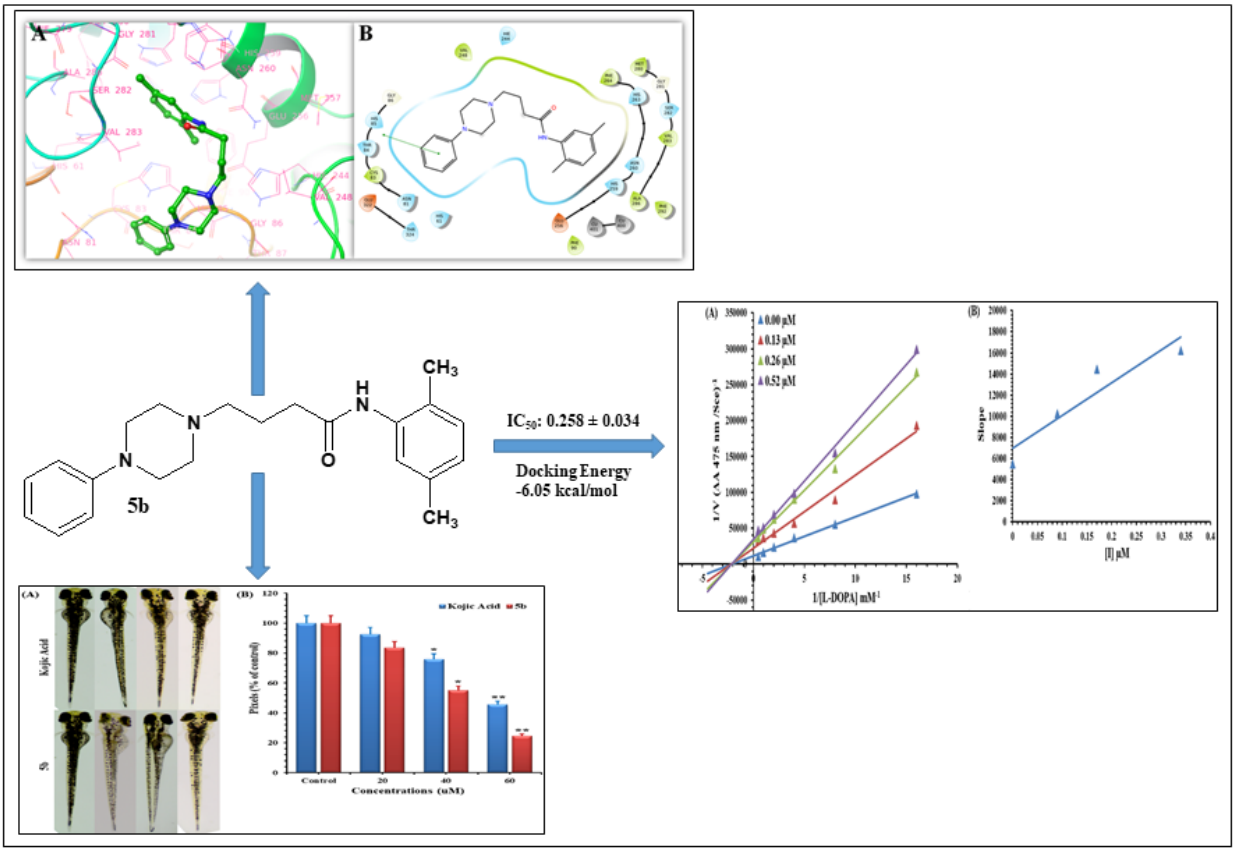
A
B
5b
IC50: 0.258 ± 0.034
Docking Energy
-6.05 kcal/mol
0.00 µM
0.13 µM
0.26 µM
0.52 µM
1/V (AA 475 nm /Sec)-1
1/[L-DOPA] mM-1
Slope
[I] µM
Kojic Acid
5b
Control
20
40
60
Concentrations (uM)

Design, synthesis and computational studies of *N*-(substituted-phenyl)-4-(4-phenyl-1-piperazinyl)butanamides as a potent anti-melanogenic and tyrosinase inhibitors

Hussain Raza[a], Muhammad Athar Abbasi[b,*], Aziz-ur-Rehman[b], Sabahat Zahra Siddiqui[b], Mubashir Hassan[c], Syed Adnan Ali Shah[d,e], Muhammad Shahid[f], Hansol Hong[a] and Sung-Yum Seo[a,*]

[a]*College of Natural Science, Department of Biological Sciences, Kongju National University, Gongju, 32588, South Korea.*

[b]*Department of Chemistry, Government College University, Lahore-54000, Pakistan.*

[c]*Institute of Molecular Biology and Biotechnology (IMBB), The University of Lahore, Lahore-54000,, Pakistan.*

[d]*Faculty of Pharmacy, Universiti Teknologi MARA Cawangan Selangor Kampus Puncak Alam, 42300 Bandar Puncak Alam, Selangor D. E., Malaysia.*

[e]*Atta-ur-Rahman Institute for Natural Products Discovery (AuRIns), Universiti Teknologi MARA Cawangan Selangor Kampus Puncak Alam, 42300 Bandar Puncak Alam, Selangor D. E., Malaysia.*

[f]*Department of Biochemistry, University of Agriculture, Faisalabad-38040, Pakistan.*

***Corresponding Authors**: [a]Prof. Dr. Sung-Yum Seo, E-mail: dnalove@kongju.ac.kr Tel: (+82)-416-8508503 and [b]Prof. Dr. Muhammad Athar Abbasi, E-mail: abbasi@gcu.edu.pk Tel: (+92)-42-111000010 Ext. 266.

Abstract

This manuscript describes the synthesis of some new *N*-(substituted-phenyl)-4-(4-phenyl-1-piperazinyl)butanamides (**5a-c**) through a facile bi-step strategy. The structures of these compounds were corroborated by their IR, EI-MS, ^{1}H-NMR, ^{13}C-NMR spectra along with CHN analysis data. The results of Mushroom tyrosinase *in vitro* inhibition revealed that all compounds were superb inhibitors of this enzyme and among them **5b** was identified as the most active compound having IC_{50} value of 0.168 ± 0.057 µM, relative to the standard (16.841 ± 1.146 µM). The kinetic analysis (K_i = 0.22 µM) of this molecule revealed that it does not competitively inhibit the tyrosinase enzyme. It also significantly reduced ($P<0.001$) the enormous amount of pigments to about 75.373% in an *in vivo* protocol, when studied on the zebrafish embryos. Moreover, the cytotoxicity of these butanamides was also profiled and it was an infered that of these molecules possess very mild cytotoxicity. So, it was consummated from the present investigation that these compounds might be utilized as less cytotoxic therapeutic agents for the betterment of skin related ailments.

Keywords: 4-Chlorobutanoyl chloride; *N*-phenylpiperazine; tyrosinase inhibition; molecular docking; depigmentation; cytotoxicity.

1. Introduction

Heterocyclic compounds are being concerned with the main domain of research for the discovery of new biologically active molecules [1]. Among the nitrogen containing heterocyclic compounds, piperazine derivatives have vide applications as pharmaceuticals [2]. The piperazine moiety is present in the structure of several compounds which exhibit wide spectrum of biological activities, including enzyme inhibition, HIV-1 inhibition, lipid peroxidation and adrenoceptor antagonism [3-6].

The compounds having a phenyl ring condensed with the piperazine heterocycle at nitrogen atom constitute a large chemical class of heterocycles. Due to lipophilic nature and small size, they have the aptitude to cross the blood-brain barrier. So, certain *N*-phenylpiperazine derivatives promote activity upon the central nervous system and are being used in the cure of numerous mental disorders, including anxiety disorders, [7] Alzheimer's disease, [8] psychosis, [9] and depression [10]. Moreover, various molecules with *N*-phenylpiperazine moiety were verified for their anticonvulsant properties and against different types of induced seizures [11-13]. Some drugs bearing phenylpiperazine skeleton have been approved by Food and Drug Administration (FDA) and itraconazole is one of the most well-known among them (Fig. 1). It was first prepared in 1984 and was made available by the FDA in 1992. It possesses a broad spectrum of activity across various fungal species [14].

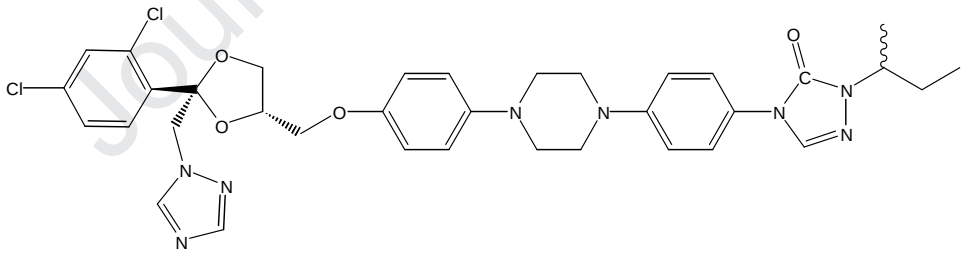

Fig. 1. Structure of itraconazole.

Ketoconazole (Fig. 2) is another FDA approved antifungal drug. It has been used for a long time with high doses, particularly for immunosuppressed patients. It has also been used for the treatment of many systemic fungal infections such as paracoccidioidomycosis, chronic mucocutaneous candidiasis, and blastomycosis [15].

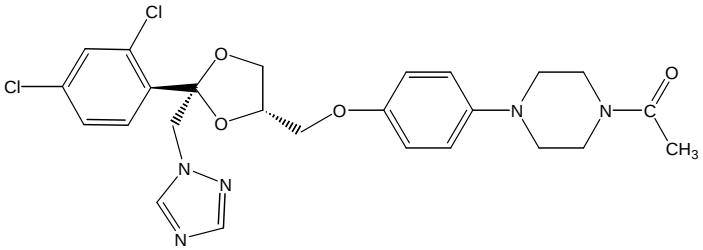

Fig. 2. Structure of ketoconazole.

Drugs containing butanamides moiety have been used in the treatment of high blood pressure, abnormal heart rhythms and sometimes chest pain [16-22].

Melanin is regulated through the process called melanogenesis. Melanin is synthesized by cells known as melanocytes, which are dendritic cells and produced from the melanoblasts. Melanoblasts are non-pigmented cells arising from the embryonic neural crest. Skin and hair follicles contain the melanin-producing cell in the basement of the epidermis. The important function of these cells is to produce the pigment melanin. These cells in skin surrounded by approximately thirty-six keratinocytes into which melanocytes transfer the prepared melanin [23].

Tyrosinase (copper bound enzyme) dispersed in plants microorganisms and animals. Tyrosinase is a pivotal enzyme with significant effects on biosynthesis and regulation of melanin. The substrate for tyrosinase (phenylalanine hydroxylase, PAH) is followed by the conversion cytosol, L-phenylalanine to tyrosine. The chemical and biological reaction, in many organisms like microbes and animals, is mono-phenols to *o*-diphenols and oxidation reaction of latter to *o*-quinones [24]. In fruits and vegetable test, surface quality and essential dietary needs are regulated through the tyrosinase. In advanced animals, humans, and plants like fungi, tyrosinase speeds up the conversion of tyrosine into melanin. Melanin not only responsible for the color but also protects the skin from UV radiations [25].

The higher quantity of melanin-pigment synthesis is responsible for different skin diseases in females and males equally such as ephelides, dark skin, acne, melasma and pregnancy spots in females [26]. Such research cheered the scientific community and industry to design and synthesize the organic compounds for the skin whitening and treatment of skin disease using tyrosinase inhibition as a target mode.

2. Experimental section

2.1. Chemistry

2.1.1. Materials and methods

Chemicals and analytical grade solvents were purchased from Sigma Aldrich, Alfa Aesar (Germany), or Merck. Pre-coated silica gel Al-plates were used for TLC. Ethyl acetate and *n*-hexane were used as solvent system. Spots were detected by UV_{254}. Gallonkamp apparatus was used to find out the melting points. Elemental analyses were performed on a Foss Heraeus CHN-O-Rapid instrument and were within ± 0.4% of the theoretical values. IR spectra (ν, cm^{-1}) were recorded by KBr pellet method in the Jasco-320-A spectrophotometer. EI-MS spectra were measured on a JEOL JMS-600H instrument. ^{1}H-NMR spectra (δ, ppm) were recorded at 600 MHz (^{13}C-NMR spectra, at 150 MHz) in DMSO-d_6 using the Bruker Advance III 600 As- cend spectrometer using BBO probe. The ^{1}H-NMR spectral peaks for interpretation are abbreviated as follows: s, singlet; d, doublet; dd, doublet of doublets; t, triplet; br.t, broad triplet; q, quartet; quint, quintet; sex, sextet; sep, septet; m, multiplet, dist, distorted.

*2.1.2. General Procedure for the synthesis of 4-Chloro-N-(substituted-phenyl)butanamides (**3a-c**)*

Substituted aniline (**2a-c**, 8.8 mmol; one in each respective reaction) was suspended in 25 mL distilled water, stirred for 30 minutes followed by the addition of 10% aqueous Na_2CO_3 to adjust pH to 9-10. Then, an equimolar quantity of 4-chlorobutanoyl chloride (**1**, 1mL, 8.8 mmol) was added with vigorous shaking, and the mixture was stirred further for four to five hours till completion of each respective reaction. Reaction progress was monitored by TLC until a single spot was achieved. During work-up, respective products were precipitated by lowering the pH up to 2.0 with conc. HCl. The precipitates of these electrophiles, 4-chloro-*N*-(substituted-phenyl)butanamides (**3a-c**) were filtered out, washed with distilled water, and air-dried.

*2.1.3. General procedure for the synthesis of N-(Substituted-phenyl)-4-(4-phenyl-1-piperazinyl)butanamides (**5a-c**)*

Phenyl piperazine (**4**, 0.5 ml; 3.08 mmol) in 10 mL *N*,*N*-dimethylformamide (DMF) was taken in 50 mL round bottomed flask and a pinch of lithium hydride was added. The reaction mixture was stirred for 30 minutes at 25 °C, for activation of **4**, followed by addition of a respective 4-chloro-*N*-(substituted-phenyl)butanamide (**3a-c**; one in each reaction). The reaction mixture was stirred for 4-5 hours till the completion of reaction in each case. The products were

precipitated by adding distilled water and got filtered, washed with distilled water, and air-dried. In this way, pure *N*-(substituted-phenyl)-4-(4-phenyl-1-piperazinyl)butanamides (**5a-c**) were obtained.

2.1.4. Structural characterization

*2.1.4.1. N-(4-Methylphenyl)-4-(4-phenyl-1-piperazinyl)butanamide (**5a**)*

Light yellow solid ; Yield: 75%; m.p. 111-112 ^{o}C; Molecular formula: $C_{21}H_{27}N_3O$; Molecular weight: 337; IR (KBr, υ/cm^{-1}): 3241 (N-H, str.), 3033 (Ar C-H str.), 1716 (C=O, str.), 1632 (Ar C=C, str.), 1588 (C=C, str.); ^{1}H-NMR and ^{13}C-NMR (Table 1); Anal. Calc. for $C_{21}H_{27}N_3O$ (337.22): C, 74.74; H, 8.06; N, 12.45. Found: C, 74.66; H, 8.15; N, 12.37; EI-MS (*m/z):* 337 $[M]^+$, 232 $[C_{14}H_{20}N_2O]^+$, 296 $[C_{18}H_{22}N_3O]^+$, 286 $[C_{17}H_{20}N_3O]^+$, 176 $[C_{11}H_{14}NO]^+$, 162 $[C_{10}H_{12}NO]^+$, 147 $[C_{10}H_{13}N]^+$, 133 $[C_9H_{11}N]^+$, 120 $[C_8H_{10}N]^+$, 107 $[C_7H_8N]^+$, 91 $[C_7H_7/C_6H_5N]^+$, 77 $[C_6H_5]^+$.

*2.1.4.2. N-(2,5-Dimethylphenyl)-4-(4-phenyl-1-piperazinyl)butanamide (**5b**)*

Light purple solid; Yield: 65%; m.p. 113-114 ^{o}C; Molecular formula: $C_{22}H_{29}N_3O$; Molecular weight: 351; IR (KBr, υ/cm^{-1}): 3239 (N-H, str.), 3030 (Ar C-H str.), 1715 (C=O, str.), 1633 (Ar C=C, str.), 1589 (C=C, str.); ^{1}H-NMR and ^{13}C-NMR (Table 2); Anal. Calc. for $C_{22}H_{29}N_3O$ (351.23): C, 75.18; H, 8.32; N, 11.96. Found: C, 75.04; H, 8.23; N, 11.99; EI-MS (*m/z):* 351 $[M]^+$, 336 $[M - CH_3]^+$, 245 $[C_{15}H_{21}N_2O]^+$, 233 $[C_{14}H_{21}N_2O]^+$, 231 $[C_{14}H_{19}N_2O]^+$, 219 $[C_{13}H_{18}N_2O]^+$, 190 $[C_{12}H_{16}NO]^+$, 175 $[C_{11}H_{15}N_2]^+$, 160 $[C_{10}H_{12}N_2]^+$, 147 $[C_{10}H_{13}N]^+$, 134 $[C_9H_{12}N]^+$, 120 $[C_8H_{10}N]^+$, 105 $[C_8H_9]^+$, 98 $[C_5H_8NO]^+$, 91 $[C_6H_5N]^+$, 77 $[C_6H_5]^+$.

*2.1.4.3. N-(3,4-Dimethylphenyl)-4-(4-phenyl-1-piperazinyl)butanamide (**5c**)*

Light yellow solid; Yield: 73%; m.p. 97-98 ^{o}C; Molecular formula: $C_{22}H_{29}N_3O$; Molecular weight: 351; IR (KBr, υ/cm^{-1}): 3242 (N-H, str.), 3048 (Ar C-H str.), 1731 (C=O, str.), 1610 (Ar C=C, str.), 1580 (C=C, str.); ^{1}H-NMR and ^{13}C-NMR (Table 3); Anal. Calc. for $C_{22}H_{29}N_3O$ (351.23): C, 75.18; H, 8.32; N, 11.96. Found: C, 75.11; H, 8.26; N, 11.88; EI-MS (*m/z):* 351 $[M]^+$, 336 $[M - CH_3]^+$, 245 $[C_{15}H_{21}N_2O]^+$, 233 $[C_{14}H_{21}N_2O]^+$, 231 $[C_{14}H_{19}N_2O]^+$, 219 $[C_{13}H_{18}N_2O]^+$, 190 $[C_{12}H_{16}NO]^+$, 175 $[C_{11}H_{15}N_2]^+$, 160 $[C_{10}H_{12}N_2]^+$, 147 $[C_{10}H_{13}N]^+$, 134 $[C_9H_{12}N]^+$, 120 $[C_8H_{10}N]^+$, 105 $[C_8H_9]^+$, 98 $[C_5H_8NO]^+$, 91 $[C_6H_5N]^+$, 77 $[C_6H_5]^+$.

Table 1

^{1}H-NMR (600 MHz, DMSO-d_6) and ^{13}C-NMR (150 MHz, DMSO-d_6) spectral data of **5a**.

No.	^{1}H-NMR (δppm) *J* (Hz)	^{13}C-NMR (δppm)	No.	^{1}H-NMR (δppm) *J* (Hz)	^{13}C-NMR (δppm)
1	9.79 (s, 1H)	171.31	3″, 5″	7.17 (br.d, *J* = 7.9 Hz, 2H,)	129.45
2	2.46 (m)*	34.45	4″	6.88 (br.d, *J* = 7.9 Hz, 1H)	119.60
3	1.80 (quint., *J* = 6.8 Hz, 2H)	25.29	1‴	-	136.67
4	3.80 (br.t, *J* = 6.8 Hz, 2H)	53.77	2‴, 6‴	7.47 (br.d, *J* = 7.8 Hz, 2H)	119.88
2′, 6′	3.33 (br.s) &	53.16	3‴, 5‴	7.53 (br.d, *J* = 8.1 Hz, 2H)	129.76
3′, 5′	2.39-2.37 (m)**	48.45	4‴	-	133.24
1″	-	147.19	7‴	2.28 (s, 3H)	20.85
2″, 6″	7.08 (br.d, *J* = 7.8 Hz, 2H)	112.56			

*Merged in the signal of DMSO d_6; ** Overall merged signals.

Table 2

^{1}H-NMR (600 MHz, DMSO-d_6) and ^{13}C-NMR (150 MHz, DMSO-d_6) spectral data of **5b**.

No.	^{1}H-NMR (δppm) *J* (Hz)	^{13}C-NMR (δppm)	No.	^{1}H-NMR (δppm) *J* (Hz)	^{13}C-NMR (δppm)
1	9.17 (s, 1H)	170.3	4″	6.77 (br.t, *J* = 7.2 Hz, 1H)	119.16
2	2.50 (m)*	34.2	1‴	-	136.7
3	1.80 (quint, *J* = 7.1	22.94	2‴	-	129.0

	Hz, 2H)				
4	3.33 (m, 2H)	57.81	3‴	7.07 (br.d, *J* = 7.6 Hz, 1H)	126.15
2′, 6′	3.13 (br.s)	53.22	5‴	-	135.3
3′, 5′	& 2.39-2.36 (m)**	48.68	6‴	7.22 (br.s, 1H,)	126.09
1″	-	151.53	4‴	6.88 (br.d, *J* = 7.4 Hz, 1H)	130
2″, 6″	6.93 (br.d, *J* = 8.1 Hz, 2H)	115.75	7‴	2.14 (s, 3H)	17.89
3″, 5″	7.21-7.19 (m, 2H)	129.34	8'''	2.23 (s, 3H)	21.01

*Merged in the signal of DMSO $d_{6;}$ ** Overall merged signals.

Table 3

^{1}H-NMR (600 MHz, DMSO-d_6) and ^{13}C-NMR (150 MHz, DMSO-d_6) spectral data of **5c**.

No.	**^{1}H-NMR (*δ*ppm) *J* (Hz)**	**^{13}C-NMR (*δ*ppm)**	**No.**	**^{1}H-NMR (*δ*ppm) *J* (Hz)**	**^{13}C-NMR (*δ*ppm)**
1	9.69 (s, 1H)	171.23	4″	6.79 (br.t, *J* = 6.7 Hz, 1H)	119.14
2	2.45 (m)*	34.80	1‴	-	137.59
3	1.77 (quint, *J* = 6.1 Hz, 2H)	22.76	2‴	7.37 (br.s, 1H)	120.80
4	3.34 (m, 2H)	57.78	3‴	-	130.95
2′, 6′	3.11 (br.s)	53.18	4‴	-	136

3′, 5′	& 2.39-2.36 (m)**	48.67	5‴	7.30 (br.d, *J* = 7.5 Hz, 1H)	129.90
1″	-	151.53	6‴	7.02 (br.d, *J* = 7.7 Hz, 1H)	117.09
2″, 6″	6.92 (br.d, *J* = 7.5 Hz, 2H)	115.74	7‴	2.15 (s, 3H)	20.05
3″, 5″	7.20 (br.t, *J* = 6.8 Hz, 2H)	129.33	8'''	2.17 (s, 3H)	19.18

*Merged in the signal of DMSO $d_{6;}$ ** Overall merged signals.

2.2. *Biology*

2.2.1. In vitro methodology

2.2.1.1. Tyrosinase inhibition

The potency of synthesized derivatives against mushroom tyrosinase (EC 1.14.18.1 Sigma Aldrich Chemical Korea) was investigated by exactly following our published method [26, 27]. In a first step, 20 mM with pH 6.8 Phosphate buffer was prepared and their 140 µL was used in each well, simultaneously 20 µL of target enzyme mushroom tyrosinase was also added from 30U/mL of stock solution. In a third step, 20 µL of the compound was poured into the assay plate. After the first incubation of 10 minutes at room temperature, the 20 µL of substrate L_DOPA was poured in each well of 96 well-plate from a stock solution of 0.85 mM, after that reaction mixture was again incubated for 20 minutes at 25 ºC. Finally, the change in absorbance was recorded at wavelength 475 nm using a microplate reader (SpectraMAX ABS, Molecular Devices, USA). For comparison and assay validation kojic acid and assay buffer was used as a positive and negative control. For IC_{50} calculations all concentration was investigated separately and repeated three times for better accuracy of results. For calculation of IC_{50} through nonlinear regression GraphPad Prism was used. By following the bellow mentioned equation % inhibition was determined.

$$Tyosinase\ \%\ inhibition\ =\ [(Blank - Sample)/Blank]\ \times 100$$

2.2.1.2. Kinetic analysis

The kinetic experiment was performed to know the behavior of compound **5b** for inhibition of tyrosinase. Range of doses was investigated for the identification of the pattern of inhibition of tyrosinase by **5b.** We examined the kinetic using our published method [28]. Totally four doses of **5b** were investigated 0.00, 0.13, 0.26 and 0.52 µM. various series of L-DOPA substrate concentrations were used from 0.0625 to 2mM for all experiments. The first incubation time and reading period was the same as presented in the anti-tyrosinase inhibition method. The maximum first velocity was determined using the primary linear phase of absorbance for 5 minutes after mixing enzyme solution at thirty seconds period. The enzyme blockage pattern was determined using the Lineweaver-Burk graph of the opposite of velocities (1/V) against the opposite of used substrate concentrations. Another chart was drawn for calculations of enzyme inhibition dissociation constant K_i through 1/V against the **5b** doses.

2.2.1.3. Hemolytic activity

For the hemolytic activity study, the bovine blood sample was collected in EDTA, diluted with (0.9% NaCl), and centrifuge the diluted sample at 1000xg for 10 minutes. The erythrocytes separated, diluted in phosphate buffer of pH 7.4, and suspension was made. 20 µL of synthesized compounds solution (10 mg/mL) in 180 µL of RBCs suspension was added and then incubated for 30 min at room temperature. PBS was used as negative control and Triton-X was taken as a positive control [29, 30]. The %age of hemolytic activity (cytotoxicity) of newly synthesized amides was calculated by using the following formula:

$$(\%)\ of\ Hemolysis = \frac{Absorbance\ of\ Sample - Absorbance\ of\ Negative\ Control}{Absorbance\ of\ Positive\ Control} \times 100$$

2.2.2. In vivo methodology

*2.2.2.1. Determination of pigmentation reducing capacity of **5b** in embryos of Zebrafish*

The animal experiments were carried out as accordance with the published methods [23, 26, 31].

2.2.2.2. Zebrafish Care and Maintenance

The selected animal zebrafishes were obtained from the local market and maintained in our fish facility laboratory for a period of thirty days. All the conditions were optimized for fish

culture as prescribed in literature for zebrafish maintains. Shrimp larvae were used as the food of fishes and they were housed in tanks made up of thermostatic material. For respiration, growth and better health air and water filtration were maintained. The fish seed was obtained using the normal procedure of fish spawning performed using the light source as a stimulator. All the animal experiments methods were confirmed by the Departmental Review Board on Kongju National University (IRB NO. 2011-2).

2.2.2.3. *Treatment and depigmentation analysis of Compound 5b*

First, the E3 medium was prepared by mixing 5 mM sodium chloride, 0.17 mM potassium chloride, 0.33 mM calcium chloride, and 0.33 mM and magnesium chloride. After that even fishes were obtained using pipette into an assay plate and poured four to five embryos in each well. In the second step, **5b** solution was prepared in 0.1% DMSO and placed into the embryos medium for nine to seventy-two hours post-fertilization. For comparison and assay confirmation kojic acid was used as a reference. After that chorion of embryos was removed and tricainemethanesulfonate MS-222 was used as anesthesia. Finally, an embryo slide was prepared using 1% methylcellulose on the entire slide and images were obtained using a stereo microscope purchased from Nikon, Japan.

2.2.3. *Computational Methodology*

2.2.3.1. Selection of mushroom tyrosinase

The 3D crystal structure of mushroom tyrosinase with PDBID: 2Y9X was repossessed form the Protein Data Bank (PDB) (https://www.rcsb.org/structure/2Y9X). The retrieved structure further undergoes for energy minimization in UCSF Chimera 1.10.1 with default parameters [32].

2.2.3.2. Grid generation and molecular docking

Before the molecular docking, the target protein was prepared using the "Protein Preparation Wizard" by the Maestro interface in the Schrödinger Suite. Initially, bond orders were assigned and hydrogen atoms were added to the target molecule. After that, the structure was then minimized to reach the converged RMSD of 0.30 Å with the OPLS_2005 force field. The binding pocket of the target protein was confirmed PDB and prior published data [25, 33]. The synthesized ligands (**5a-c**) were sketched in a 2D sketcher in Schrödinger Suite and saved in

the Maestro interface for docking experiments. The molecular docking experiment was carried out between all ligands and selected target structures through the Glide docking protocol [34]. The generated docking complexes (3D/2D) were examined on the basis of energy values and binding interaction profiles. Throughout the docking simulations, both partial flexibility and full flexibility around the active site residues are performed by Glide/SP/XP and induced fit docking (IFD) approaches [35].

2.2.3.3. Molecular Dynamics

To understand the protein backbone stability in the docking complex, a molecular dynamics simulation experiment was performed through the Desmond simulation package of Schrödinger [36]. In all runs, the NPT ensemble was applied to have a temperature of 300 K and pressure of 1 bar. The simulation time of 100 ns having relaxation time 1 ps was adjusted throughout the simulation experiment with the OPLS_2005 force field parameter [37]. The long-range electrostatic interactions were calculated using the particle mesh Ewald (PME) method [38]. The cutoff radius in coloumb interactions was fixed at 9.0 Å, whereas, water molecules were explained using a simple point charge (SPC) model [39]. The Martyna-Tuckerman-Klein chain coupling scheme [40] with a coupling constant of 2.0 ps was used for pressure control and the Nosé-Hoover chain coupling scheme for temperature control. To analyze the behavior and interactions between the ligands and protein, we used the Simulation Interactions Diagram tool implemented in the Desmond molecular dynamics package.

3. **Results and Discussion**

3.1. Chemistry

The synthetic procedures adopted to obtain the target compounds are outlined in scheme 1 and conditions of reactions are described in the experimental section. Treatment of 4-chlorobutanoyl chloride (**1**) with three different *N*-substituted anilines (**2a-c**) gave the respective electrophiles, 4-chloro-*N*-(substituted-phenyl)butanamide (**3a-c**). *N*-Phenylpiperazine (**4**) was taken in DMF and lithium hydride base added to activate this nucleophilic compound, and then the newly synthesized electrophiles, **3a-c**, were reacted with **4** to transform it into *N*-(substituted-phenyl)-4-(4-phenyl-1-piperazinyl)butanamides (**5a-c**). The structures of the products were deduced from their elemental analysis and spectral data. For example, the molecular mass of **5a** was accounted by molecular ion peak in EI-MS spectrum at *m/z* 337 (Fig. S1) and molecular

formula, $C_{21}H_{27}N_3O$, was established through CHN analysis data. The count of a number of protons and the number of carbon resonances in its ^{1}H-NMR and ^{13}C-NMR spectrum, respectively, was also in agreement with the suggested molecular formula. The most downfield singlet in its ^{1}H-NMR spectrum at δ 9.79 (NH-CO-1) was an attribute of amidic heteroatom proton. 4-Methylphenyl moiety was clearly corroborated by two *ortho*-coupled doublets in aromatic region, appearing at δ 7.53 (br.d, J = 8.1 Hz, 2H, H-3''' & H-5'''), and 7.47 (br.d, J = 7.8 Hz, 2H, H-2''' & H-6''') along with a discrete singlet for a methyl group in aliphatic region at δ 2.28 (s, 3H, CH_3-7'''). The distinct resonances for a symmetrical piperazine ring were not observed, most probably, due to ring flipping, and it was collectively characterized by a broad singlet δ 3.33 and a multiplet signal at δ 2.39-2.37 for all its four methylenes. The phenyl group attached with nitrogen of the piperazine ring was represented by three peculiar signals at δ 7.17 (br.d, J = 7.9 Hz, 2H, H-3'' & H-5''), 7.08 (br.d, J = 7.8 Hz, 2H, H-2'' & H-6''), and 6.88 (br.d, J = 7.9, 1H, H-4''). Peaks at δ 3.80 (br.t, J = 6.8 Hz, 2H, CH_2-4), 2.46 (m, merged in the signal of DMSO-d_6, CH_2-2) and 1.80 (quint, J = 6.8, 2H, CH_2-3) exposed the presence of a butanamido group (Fig. S2). The ^{13}C-NMR spectrum demonstrated overall fifteen carbon resonances, because some duplets for magnetically equivalent carbons were reducing the total resonances of the molecule. The carbons of 4-methylphenyl moiety appeared at δ 136.67 (C-1'''), 133.24 (C-4'''), 129.76 (C-3''' & C-5'''), 119.88 (C-2''' & C-6'''), and 20.85 (C7'''). Two resonances for piperazine ring were observed at δ 53.16 (C2' & C6'), and 48.45 (C3' & C5') while phenyl group attached with this piperazine was evident from four peaks at δ 147.19 (C-1''), 129.45 (C-3'' & C-5''), 119.60 (C4''), 112.56 (C-2'' & C-6'') [41]. The linking butanamide moiety was endorsed by four resonances at δ 171.31 (C-1), 53.77 (C-4), 34.45 (C-2), and 25.29 (C-3). Various mass fragments (shown in the experimental section) of this molecule also thoroughly supported these assignments. So, based on all these cumulative evidence, the structure of **5a** was confirmed and it was named as *N*-(4-methylphenyl)-4-(4-phenyl-1-piperazinyl)butanamide. Similarly, the structures of other derivatives were also characterized by a similar strategy.

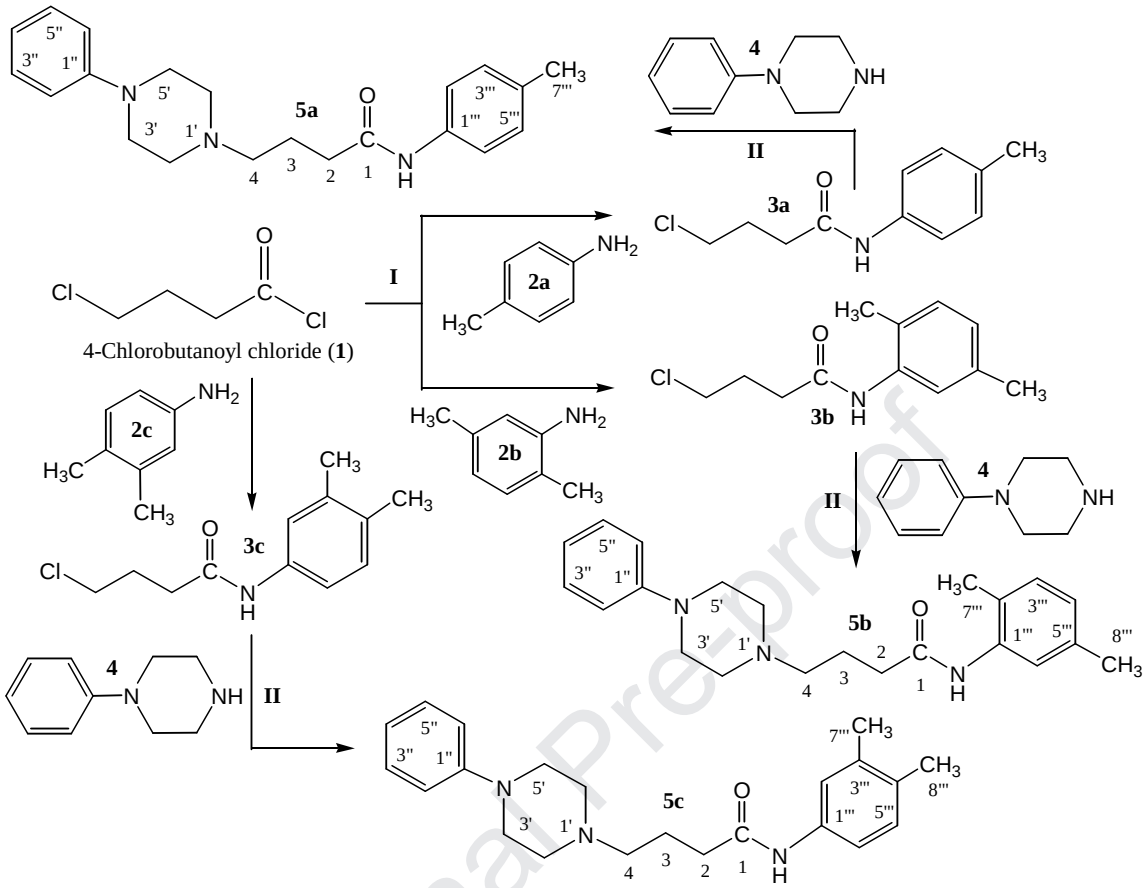

Scheme 1. Outline for the synthesis of *N*-(substituted-phenyl)-4-(4-phenyl-1-piperazinyl)butanamides. **Reagents & Conditions**: (I) Aq. Na_2CO_3 soln./pH 9-10/stirring at RT for 3-4 hrs. (II) Acetonitrile/K_2CO_3/refluxing of **4** for 0.5 hrs for its activation, followed by addition of respective electrophile (**3a-c**), and then refluxing for 4-5 hrs.

3.2. Biology

3.2.1. Enzyme inhibition and structure-activity relationship

The synthesized compounds (**5a-c**) were screened to confirm their importance as inhibitors of the tyrosinase enzyme. Kojic acid was used as a standard for comparing results, and estimates of the half-maximum inhibitory concentration (IC_{50}) are summarized in (Table 4). Interestingly, all synthesized compounds showed potent inhibition against mushroom tyrosinase compared to kojic acid. Compound **5b** (0.258 ± 0.024) was the dominant tyrosinase inhibitor compared to other compounds in the series. The presence of two methyl groups at 2 and 5 positions of the benzene ring results in the best activity of tyrosinase. The compound **5b** interacts

strongly and occupies the whole pocket of the receptor. The compound **5c** exhibited moderately inhibitory activity in the comparison of other compounds due to change in position of a methyl group at 3 and 4 position of benzene ring as compared to **5b**. It poorly interacted with enzyme and unable to occupy the pocket of the receptor. The **5a** compound was the second potent inhibitor due to the presence of only one methyl group at *para*-position, however, the substitution of the methyl group at *para*-position decreases the steric hindrance which increases the inhibitory effect.

Table 4

IC_{50} values of compounds (**5a-c**) were calculated by nonlinear regression using GraphPad Prism 5.0.

Compound	**Tyrosinase activity IC_{50} ± SEM (µM)**
5a	0.307 ± 0.043
5b	0.258 ± 0.034
5c	0.421 ± 0.052
Kojic Acid	16.841 ± 1.146

SEM= Standard error of the mean (n=3).

3.2.2. Kinetic analysis

Based on our results, the most potent compound **5b** is selected to determine the type of tyrosinase inhibition and the inhibition constant. The potential of this compound to inhibit the free enzyme and the enzyme-substrate complex was determined as an EI or ESI constant. The kinetic studies of the enzyme by the Lineweaver-Burk plot of 1/V versus 1/[S] in the presence of different concentrations of the compound revealed a series of straight lines (Fig. 3A). The results of **5b** showed that the compound cuts in the second quadrant. The analysis showed that V_{max} decreased to new, increasing doses of inhibitors while K_m remained the same. This behavior indicates that **5b** does not competitively inhibit tyrosinase to form the enzyme-inhibitor complex. Secondary plots of slope versus inhibitor concentrations showed dissociation constant of an enzyme inhibitor (K_i) (Fig. 3B).

The kinetic results are presented in the Table 5. (Kinetic parameter table).

Table 5

Kinetic parameters of the mushroom tyrosinase for L-DOPA activity in the presence of various concentration of **5b**.

Concentration (µM)	V_{max} (ΔA /Sec)	K_m (mM)	Inhibition Type	K_i (µM)
0.00	9.52×10^{-5}	0.38	Non-Competitive	0.22
0.13	2.99×10^{-5}	0.38		
0.26	2.76×10^{-5}	0.38		
0.52	2.13×10^{-5}	0.38		

V_{max} is the reaction velocity, Km is the Michaelis-Menten constant**,** K_i is the EI dissociation constant**.**

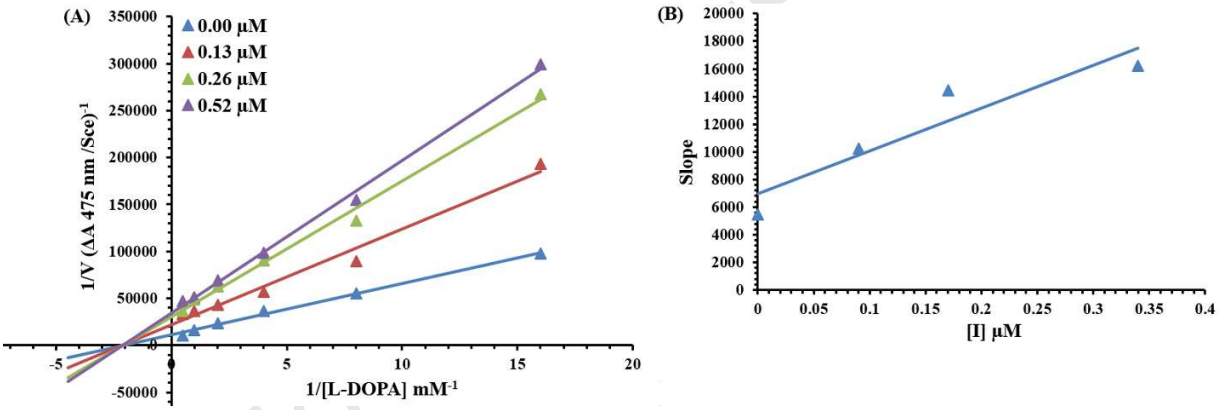

Fig. 3. Lineweaver–Burk plots for inhibition of tyrosinase in the presence of Compound **5b**. (A) Concentrations of **5b** were 0.00, 0.13, 0.26 and 0.52 µM, respectively. L-DOPA Substrate Concentrations were 0.0625, 0.125, 0.25, 0.5, 1 and 2 mM, respectively. (B) The insets are a plot of the concentrations of **5b** slope versus inhibitor to determine the inhibition constant. Lines were drawn using linear least squares fit.

3.2.3. Hemolytic activity

All the synthesized compounds, **5a-c**, were also subjected to hemolytic assay to find out their cytotoxicity profile. Results of percentage hemolysis are shown in (Table 6). Our results showed that all these have very low cytotoxicity towards the red blood cell membrane. Maximum membrane toxicity was shown by compound **5c** which is only 6.54 ± 0.04% relative

to Triton-X having a value of 87.67 ± 0.03%. The minimum toxicity was recorded in **5b** (2.54 ± 0.01%) while **5a** exhibited 2.85 ± 0.02% hemolysis.

Table 6

Cytotoxicity studies of the synthesized amides, **5a-c**.

Compound	% Hemolysis
5a	2.85 ± 0.02
5b	2.54 ± 0.01
5c	6.54 ± 0.04
Triton X	87.67 ± 0.03
Note: PBS (% Hemolysis) = 1.03 ± 0.01.	

3.2.4. In vivo depigmentation zebrafish analysis

Zebrafish is a vital research model against various diseases, due to gene makeup similarity with humans [23]. Owing to these benefits, the zebrafish seeds were used to determine the depigmentation efficacy of **5b** through *in vivo* assay. The inhibition efficacy of **5b** on the coloring of zebrafish was investigated with the treatment of 20, 40 and 60 µM of inhibitor **5b** and equal doses were tested for kojic acid, and for the negative control, embryos were treated without any compound only with E3 medium embryos were treated. The pigment level of zebrafish significantly decreased $P<0.001$, (Fig. 4A, B) to about 75.373% while positive control kojic acid showed 54.473% at 60 µM. Additionally, inhibitor **5b** exhibited good depigmenting effects at 40 and 60 µM doses, relative to those of kojic acid.

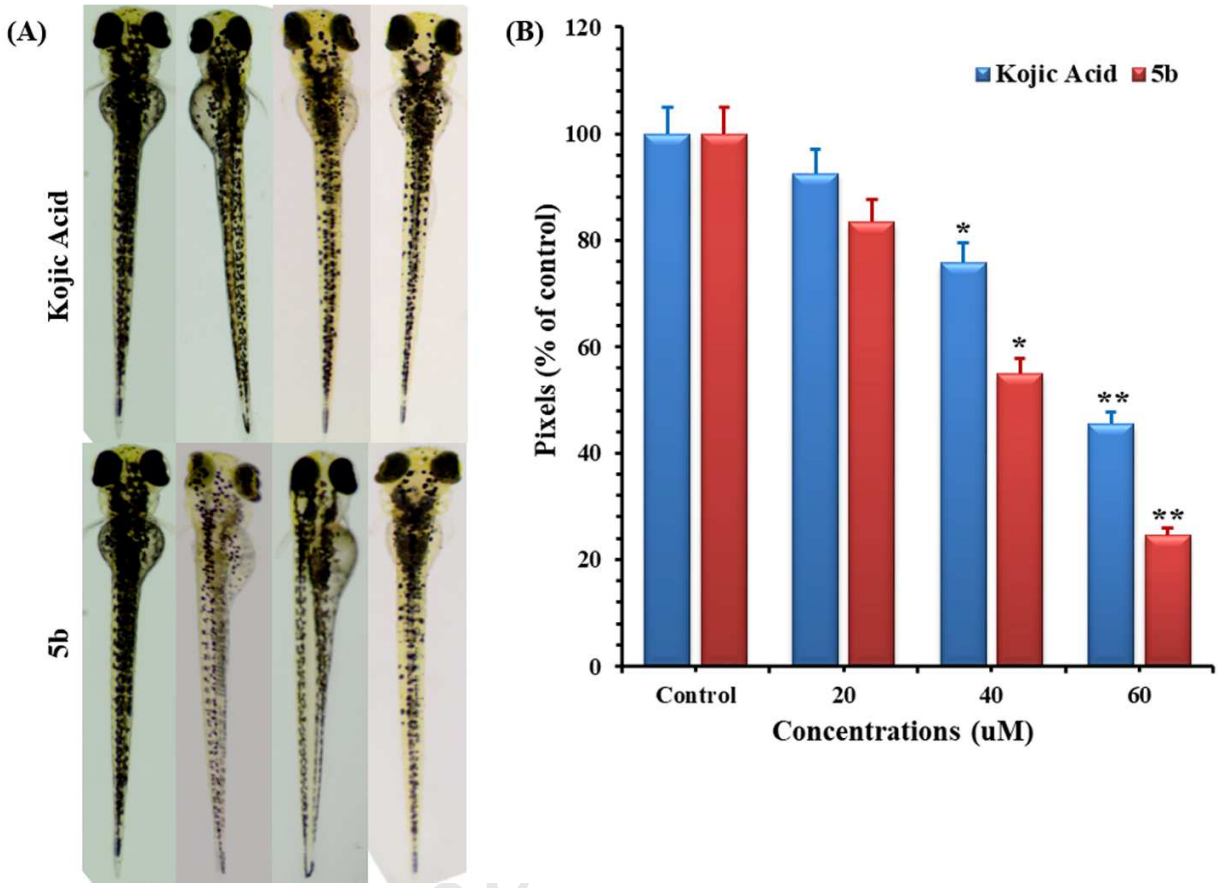

Fig. 4. Depigmentation efficacy of **5b** in zebrafish (A) showed the melanin amount decrease in zebrafish at different doses. (B) Graphically comparison of melanin amount of **5b** and standard kojic acid. The amount of melanin was measured using ImageJ software. *P<0.05; **P<0.001. The results were compared using analysis of variance (ANOVA) followed by a Dunnett test.

3.2.5. Molecular docking analysis

3.2.5.1. Binding energy evaluation of synthesized compounds

To predict the best conformational position within the active region of tyrosinase, all compounds were undergoes a docking procedure. The predicted docked complexes were examined based on docking energy values (kcal/mol), hydrogen and hydrophobic bonding pattern. The docking results showed that all the synthesized ligands (**5a-c**) were bind within the active site of the target protein with different conformational poses and energy values (kcal/mol), respectively. The binding pattern of all synthesized compounds showed their similar conformational behavior within the active region of the target protein (Fig. 5A). The compound **5a** exhibited -6.38 (kcal/mol), whereas, **5b** and **5c** possessed -6.05 and -5.90 kcal/mol,

respectively (Fig. 5B). It was observed that all ligands exhibited similar chemical skeleton, therefore, no big energy value difference was observed in all docking results.

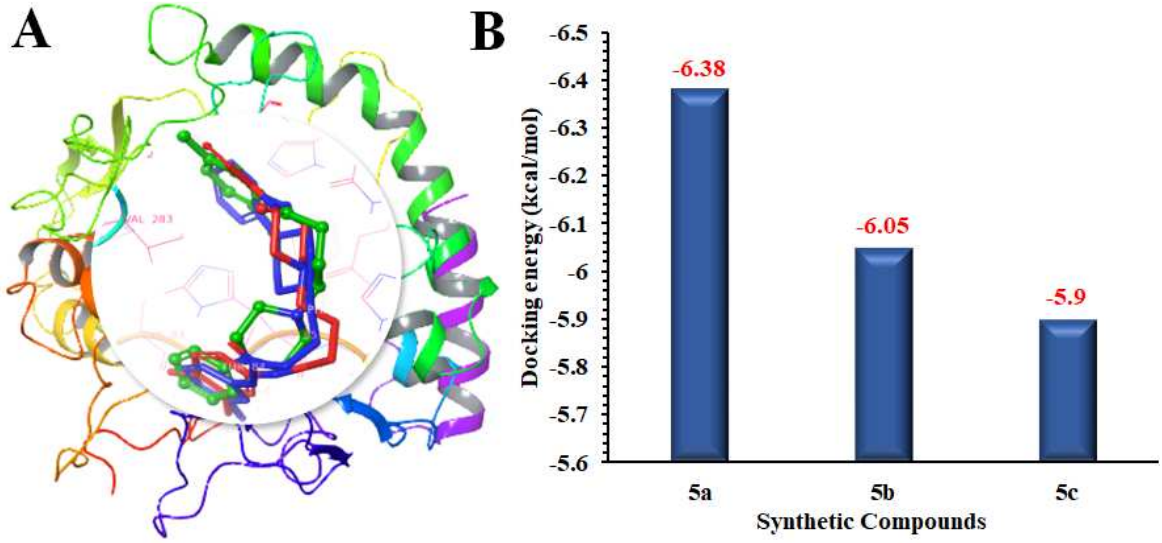

Fig. 5 (A, B). Docking complexes of **5a-c** with binding affinities (kcal/mol).

3.2.5.2. Binding analysis of ligands against tyrosinase

The detail docking analysis of **5b** exhibited a single π-π interaction. The 3D and 2D depictions of most active compound **5b** are mentioned in (Fig. 6A, B). Furthermore, in **5a** docking complex, one hydrogen and a couple of π-π interactions were observed at His244, Phe264, and His85, respectively. The carbonyl oxygen atom formed hydrogen bond whereas, dimethyl benzene and other benzene rings were interacted with His85 and Phe264, respectively. Similarly, in **5c**-docking complex one hydrogen and three hydrophobic interactions were observed as mentioned in (Fig. 7A, B). Prior docking studies showed that the significance of these amino acids in bonding with other tyrosinase inhibitors supports our docking results [24-26, 33].

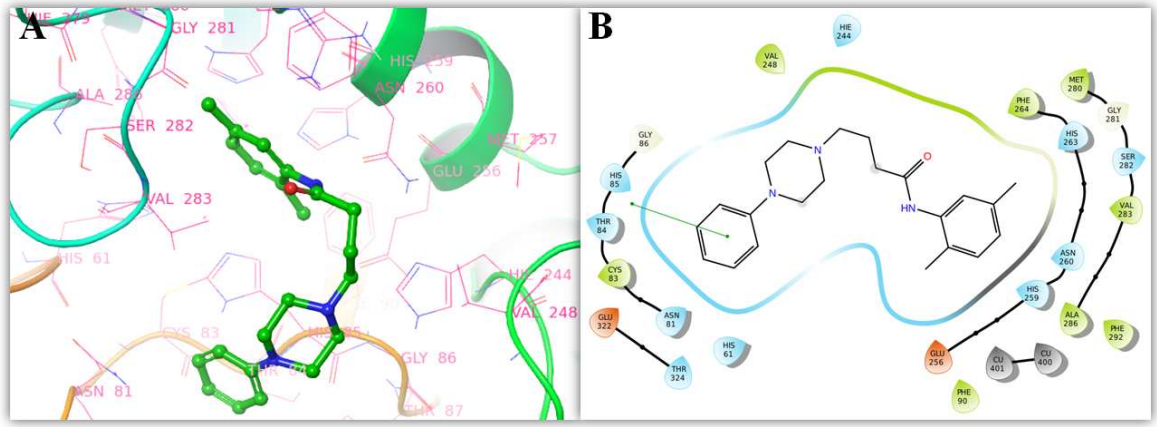

Fig. 6. 3D and 2D-docking depiction of **5b** complex against tyrosinase.

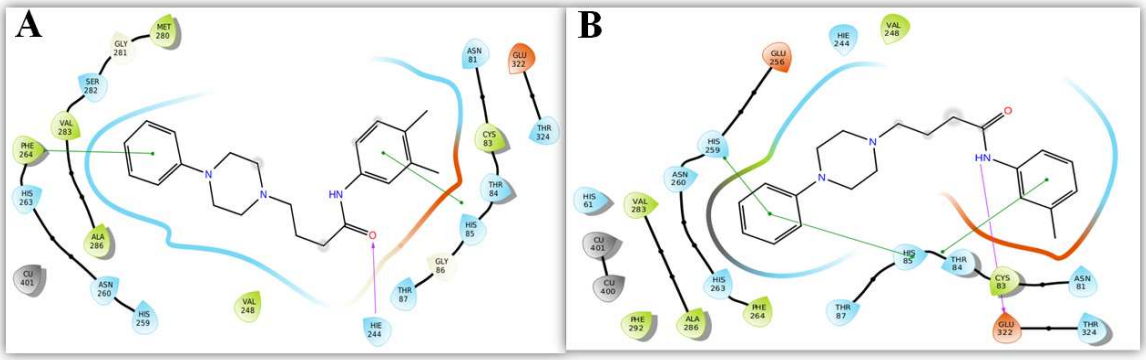

Fig. 7 (A and B). 2D-docking depiction of **5a** and **5c** complex against tyrosinase.

3.2.6. Molecular dynamic simulations

3.2.6.1. RMSD and RMSF analysis

To assess the residual flexibility of receptor through MD simulation RMSD and RMSF graphs were generated to evaluate the protein structural behavior. The RMSD graph result of **5b** interprets the protein residual deviation in a 100 ns simulation time frame. Initially, the graph line showed an increasing trend from 0-40 ns having RMSD value range from 0.25 and 2.00 Å for backbone residues. The generated RMSD graph showed little stability from 20 to 40 ns, however, the graph fluctuations were higher at 40 ns compared to 10, 20 and 30 ns. After that, the promising result was observed and the graph line remained stable until 100 ns having constant RMSD value 2.00 Å. The overall RMSD analysis showed that fluctuations in a graph in the whole simulation are within the standard range of RMSD 1-3 Å which showed backbone stability in docking (Fig. 8). The RMSF is useful for characterizing local changes along with the protein structure. The generated plot indicated protein behavior fluctuations during the

simulation in Cα and backbone residues. The overall results showed that N- and C-terminals loop regions showed little fluctuations whereas, residues around 170-200 depicted high fluctuations in 100 ns simulation (Fig. 9).

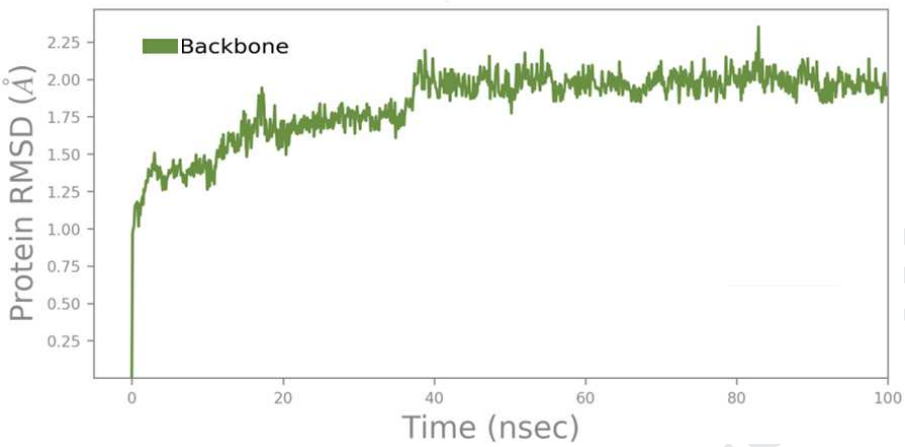

Fig. 8. RMSD graph of **5b** docking complex at 100 ns.

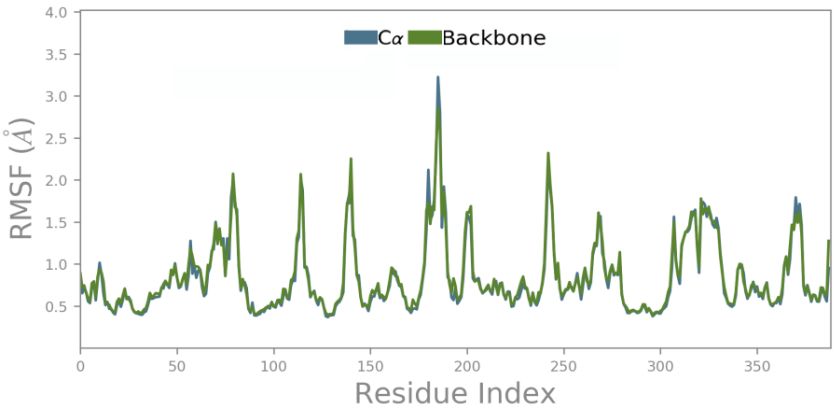

Fig. 9. RMSF graph of **5b** docking complex at 100 ns.

4. Conclusion

In summary, all the newly synthesized *N*-(substituted-phenyl)-4-(4-phenyl-1-piperazinyl)butanamide derivatives (**5a-c**) demonstrated superb tyrosinase inhibitory activity. Among them, the compound **5b** displayed excellent activity with an IC_{50} value (0.258 ± 0.024 µM) relative to that of standard kojic acid (16.841 ± 1.146 µM). *In silico* computational studies of all compounds also augmented the *in vitro* analysis, whereby these molecules exhibited strong interactions with the target protein and formed stable complexes with tyrosinase. *In vivo* anti-melenogenic results also exposed that **5b** significantly reduced the amount of pigments, without

any damage to the zebrafish. These butanamides also exhibited mild cytotoxicity towards red blood cell membranes. So, it was concluded from the whole study that these molecules were good therapeutic agents, in general. However, **5b**, in particular, might serve as a superb tyrosinase inhibitor and an excellent anti-melanogenic agent for the treatment of skin related ailments.

Author contribution statement

Hussain Raza: Performed *in vitro* and *in vivo* experiments and wrote the initial draft of manuscript. **Sabahat Zahra Siddiqui** and **Aziz-ur-Rehman:** Synthesized the chemical compounds. **Mubashir Hassan:** Performed the *in silico* computational experiments. **Syed Adnan Ali Shah:** Done spectral analysis and characterization of compounds. **Muhammad Shahid:** Performed cytotoxicity experiments. **Hansol Hong:** Helped in the analysis of data. **Muhammad Athar Abbasi** and **Sung-Yum Seo:** Facilitated and supervised the whole study. Also checked and approved the final draft of this manuscript.

Conflicts of interest

The authors declare no conflict of interests.

Acknowledgement

The present study was supported by Basic Science Research Program through the National Research Foundation of Korea (NRF) funded by the Ministry of Education (2017R1D1A1B03034948).

References

[1] M.A. Abbasi, G. Hussain, A. Rehman, S.Z. Siddiqui, S.A. Shah, M.A. Lodhi, F.A. Khan, M. Ashraf, Q. Ain, I. Ahmad, R. Malik, Synthesis of some unique carbamate derivatives bearing 2-Furoyl-1-piperazine as valuable therapeutic agents, Acta Chim. Slov. 64 (2017) 159-169. https://doi.org/10.17344/acsi.2016.2986.

[2] W.R. Roderick, H.J. Platte, C.B. Pollard, Derivatives of Piperazine. XXXV. 1a Synthesis of 2-Phenylpiperazine and Some Derivatives, J. Med. Chem. 9 (1966) 181-185. https://doi.org/10.1021/jm00320a005.

[3] J.R. Tagat, S.W. McCombie, R.W. Steensma, S.I. Lin, D.V. Nazareno, B. Baroudy, N. Vantuno, S. Xu, J. Liu, Piperazine-based CCR5 antagonists as HIV-1 inhibitors. I: 2 (S)-methyl piperazine as a key pharmacophore element, Bioorg. Med. Chem. Lett. 11 (2001) 2143-2146. https://doi.org/10.1016/s0960-894x(01)00381-x.

[4] J.A. Kozlowski, G. Zhou, J.R. Tagat, S.I. Lin, S.W. McCombie, V.B. Ruperto, R.A. Duffy, R.A. McQuade, G. Crosby Jr, L.A. Taylor, W. Billard, Substituted 2-(R)-methyl piperazines as muscarinic M2 selective ligands, Bioorg. Med. Chem. Lett. 12 (2002) 791-794. https://doi.org/10.1016/s0960-894x(02)00023-9.

[5] P.E. Chabrier, M. Auguet, B. Spinnewyn, S. Auvin, S. Cornet, C. Demerlé-Pallardy, C. Guilmard-Favre, J.G. Marin, B. Pignol, V. Gillard-Roubert, C. Roussillot-Charnet, BN 80933, a dual inhibitor of neuronal nitric oxide synthase and lipid peroxidation: a promising neuroprotective strategy, Proc. Natl. Acad. Sci. 96 (1999) 10824-10829. https://doi.org/10.1073/pnas.96.19.10824.

[6] R. Barbaro, L. Betti, M. Botta, F. Corelli, G. Giannaccini, L. Maccari, F. Manetti, G. Strappaghetti, S. Corsano, Synthesis and biological activity of new 1, 4-benzodioxan-arylpiperazine derivatives. Further validation of a pharmacophore model for α1-adrenoceptor antagonists, Bioorg. Med. Chem. 10 (2002) 361-369. https://doi.org/10.1016/s0968-0896(01)00286-3.

[7] M.A. Katzman, Aripiprazole: a clinical review of its use for the treatment of anxiety disorders and anxiety as a comorbidity in mental illness, J. Affective Disord. 128 (2011) 11-20. https://doi.org/10.1016/s0165-0327(11)70004-0.

[8] C.T. Sadashiva, J.N. Chandra, K.C. Ponnappa, T.V. Gowda, K.S. Rangappa, Synthesis and efficacy of 1-[bis (4-fluorophenyl)-methyl] piperazine derivatives for

acetylcholinesterase inhibition, as a stimulant of central cholinergic neurotransmission in Alzheimer's disease, Bioorg. Med. Chem. Lett. 16 (2006) 3932-3936. https://doi.org/10.1016/j.bmcl.2006.05.030

[9] R. Menegatti, A.C. Cunha, V.F. Ferreira, E.F. Perreira, A. El-Nabawi, A.T. Eldefrawi, E.X. Albuquerque, G. Neves, S.M. Rates, C.A. Fraga, E.J. Barreiro, Design, synthesis and pharmacological profile of novel dopamine D2 receptor ligands, Bioorg. Med. Chem. 11 (2003) 4807-4813. https://doi.org/10.1016/s0968-0896(03)00487-5.

[10] G.I. Papakostas, M. Fava, A meta-analysis of clinical trials comparing the serotonin (5HT)-2 receptor antagonists trazodone and nefazodone with selective serotonin reuptake inhibitors for the treatment of major depressive disorder, Eur. Psychiatry 22 (2007) 444-447. https://doi.org/10.1016/j.eurpsy.2007.01.1220.

[11] J. Obniska, A. Zagorska, Synthesis and anticonvulsant properties of new N-[(4-arylpiperazin-1-yl)-methyl] derivatives of 3-aryl pyrrolidine-2, 5-dione and 2-aza-spiro [4.4] nonane-1, 3-dione, Il Farmaco 58 (2003) 1227-1234. https://doi.org/10.1016/s0014-827x(03)00187-3.

[12] B. Malawska, K. Kulig, M. Ciechanowicz□Rutkowska, Search for New Anticonvulsant Compounds, Part 2. Structure□Activity Relationship Studies of New N□Substituted Amides of α□Piperazine□γ□Hydroxybutyric Acid as Active Anticonvulsants, Arch. Pharm. 330 (1997) 91-99. https://doi.org/10.1002/ardp.19973300403.

[13] B. Malawska, A. Zejc, Search for new anticonvulsant compounds. Part 1: Synthesis, physicochemical and anticonvulsant properties of new derivatives of alpha-amino-gamma-phthalimidobutyric acid, Pharmazie 50 (1995) 722-725. https://doi.org/10.1002/chin.199610215.

[14] J. Kim, J.Y. Tang, R. Gong, J. Kim, J.J. Lee, K.V. Clemons, C.R. Chong, K.S. Chang, M. Fereshteh, D. Gardner, T. Reya, Itraconazole, a commonly used antifungal that inhibits Hedgehog pathway activity and cancer growth, Cancer cell 17 (2010) 388-399. https://doi.org/10.1016/j.ccr.2010.02.027.

[15] D.S. Loose, P.B. Kan, M.A. Hirst, R.A. Marcus, D. Feldman, Ketoconazole blocks adrenal steroidogenesis by inhibiting cytochrome P450-dependent enzymes, J. Clin. Invest. 71 (1983) 1495-1499. https://doi.org/10.1172/jci110903.

[16] A.N. Chatterji, A randomized crossover comparison of acebutolol and methyldopa in the treatment of mild to moderate essential hypertension, Curr. Med. Res. Opin. 5 (1978) 675-681. https://doi.org/10.1185/03007997809110206.

[17] B.N. Singh, W.R. Thoden, A. Ward, Acebutolol. A review of its pharmacological properties and therapeutic efficacy in hypertension, angina pectoris and arrhythmia, Drugs 29 (1985) 531-569. https://doi.org/10.2165/00003495-198529060-00003.

[18] A.H. Gradman, R.A. Winkle, J.W. Fitzgerald, P.J. Meffin, J. Stoner 3rd, P.A. Bell, D.C. Harrison, Suppression of premature ventricular contractions by acebutolol, Circulation 55 (1977) 785-791. https://doi.org/10.1161/01.cir.55.5.785.

[19] L. Hansson, G. Berglund, O. Andersson, M. Holm, Controlled trial of acebutolol in hypertension, Eur. J. Clin. Pharmacol. 12 (1977) 89-92. https://doi.org/10.1007/bf00645127.

[20] R.N. Hanson, B.L. Holman, M.A. Davis, Synthesis and biologic distribution of radioiodinated. beta.-adrenergic antagonists, J. Med. Chem. 21 (1978) 830-833. https://doi.org/10.1021/jm00206a025.

[21] B. Basil, J.R. Clark, E.C. Coffee, R. Jordan, A.H. Loveless, D.L. Pain, K.R. Wooldridge, New series of cardioselective adrenergic. beta.-receptor blocking compounds. 1-(2-Acyl-4-acylaminophenoxy)-3-isopropylaminopropan-2-ols, J. Med. Chem. 19 (1976) 399-402. https://doi.org/10.1021/jm00225a012.

[22] B. Flouvat, A. Roux, N.P. Chau, M. Viallet, X. Andre-Fouet, R. Woehrle, J. Gregoire, Pharmacokinetics and bioavailability of diacetolol, the main metabolite of acebutolol, Eur. J. Clin. Pharmacol. 19 (1981) 287-292. https://doi.org/10.1007/bf00562806.

[23] Q. Abbas, Z. Ashraf, M. Hassan, H. Nadeem, M. Latif, S. Afzal, S.Y. Seo, Development of highly potent melanogenesis inhibitor by in vitro, in vivo and computational studies, Drug Des., Dev. Ther. 11 (2017) 2029-2046. https://doi.org/10.2147/dddt.s137550.

[24] A. Saeed, P.A. Mahesar, P.A. Channar, Q. Abbas, F.A. Larik, M. Hassan, H. Raza, S.Y. Seo, Synthesis, molecular docking studies of coumarinyl-pyrazolinyl substituted thiazoles as non-competitive inhibitors of mushroom tyrosinase, Bioorg. Chem. 74 (2017) 187-196. https://doi.org/10.1016/j.bioorg.2017.08.002.

[25] F.A. Larik, A. Saeed, P.A. Channar, U. Muqadar, Q. Abbas, M. Hassan, S.Y. Seo, M. Bolte, Design, synthesis, kinetic mechanism and molecular docking studies of novel 1-

pentanoyl-3-arylthioureas as inhibitors of mushroom tyrosinase and free radical scavengers, Eur. J. Med. Chem. 141 (2017) 273-281. https://doi.org/10.1016/j.ejmech.2017.09.059.

[26] Q. Abbas, H. Raza, M. Hassan, A.R. Phull, S.J. Kim, S.Y. Seo, Acetazolamide inhibits the level of tyrosinase and melanin: an enzyme kinetic, in vitro, in vivo, and in silico studies, Chem. Biodivers. 14 (2017) e1700117. https://doi.org/10.1002/cbdv.201700117.

[27] R. Qamar, A. Saeed, F.A. Larik, Q. Abbas, M. Hassan, H. Raza, S.Y. Seo, Novel 1, 3□oxazine□tetrazole hybrids as mushroom tyrosinase inhibitors and free radical scavengers: Synthesis, kinetic mechanism, and molecular docking studies, Chem. Biol. Drug Des. 93 (2019) 123-131. https://doi.org/10.1111/cbdd.13352.

[28] N.C. Dige, P.G. Mahajan, H. Raza, M. Hassan, B.D. Vanjare, H. Hong, K.H. Lee, S.Y. Seo, Ultrasound mediated efficient synthesis of new 4-oxoquinazolin-3 (4H)-yl) furan-2-carboxamides as potent tyrosinase inhibitors: Mechanistic approach through chemoinformatics and molecular docking studies, Bioorg. Chem. 92 (2019) 103201. https://doi.org/10.1016/j.bioorg.2019.103201.

[29] P. Sharma, J.D. Sharma, In vitro hemolysis of human erythrocytes—by plant extracts with antiplasmodial activity, J. Ethnopharmacol. 74 (2001) 239-243. https://doi.org/10.1016/s0378-8741(00)00370-6.

[30] H. Raza, M.A. Abbasi, S.Z. Siddiqui, M. Hassan, Q. Abbas, H. Hong, S.A. Shah, M. Shahid, S.Y. Seo, Synthesis, molecular docking, dynamic simulations, kinetic mechanism, cytotoxicity evaluation of N-(substituted-phenyl)-4-{(4-[(E)-3-phenyl-2-propenyl]-1-piperazinyl} butanamides as tyrosinase and melanin inhibitors: In vitro, in vivo and in silico approaches, Bioorg. Chem. 94 (2020) 103445. https://doi.org/10.1016/j.bioorg.2019.103445.

[31] T.Y. Choi, J.H. Kim, D.H. Ko, C.H. Kim, J.S. Hwang, S. Ahn, S.Y. Kim, C.D. Kim, J.H. Lee, T.J. Yoon, Zebrafish as a new model for phenotype□based screening of melanogenic regulatory compounds, Pigment Cell Res. 20 (2007) 120-127. https://doi.org/10.1111/j.1600-0749.2007.00365.x.

[32] E.F. Pettersen, T.D. Goddard, C.C. Huang, G.S. Couch, D.M. Greenblatt, E.C. Meng, T.E. Ferrin, UCSF Chimera—a visualization system for exploratory research and analysis, J. Comput. Chem. 13 (2004) 1605-1612. https://doi.org/10.1002/jcc.20084.

[33] M. Hassan, Z. Ashraf, Q. Abbas, H. Raza, S.Y. Seo, Exploration of novel human tyrosinase inhibitors by molecular modeling, docking and simulation studies, Interdiscip. Sci.: Comput. Life Sci. 10 (2018) 68-80. https://doi.org/10.1007/s12539-016-0171-x.

[34] R.A. Friesner, R.B. Murphy, M.P. Repasky, L.L. Frye, J.R. Greenwood, T.A. Halgren, P.C. Sanschagrin, D.T. Mainz, Extra precision glide: Docking and scoring incorporating a model of hydrophobic enclosure for protein− ligand complexes, J. Med. Chem. 49 (2006) 6177-6196. https://doi.org/10.1021/jm051256o.

[35] R. Farid, T. Day, R.A. Friesner, R.A. Pearlstein, New insights about HERG blockade obtained from protein modeling, potential energy mapping, and docking studies, Bioorg. Med. Chem. 14 (2006) 3160-3173. https://doi.org/10.1016/j.bmc.2005.12.032.

[36] K.J. Bowers, D.E. Chow, H. Xu, R.O. Dror, M.P. Eastwood, B.A. Gregersen, J.L. Klepeis, I. Kolossvary, M.A. Moraes, F.D. Sacerdoti, J.K. Salmon, Scalable algorithms for molecular dynamics simulations on commodity clusters, InSC'06: Proceedings of the 2006 ACM/IEEE Conference on Supercomputing, IEEE, 2006 pp. 43–43. https://doi.org/10.1145/1188455.1188544.

[37] J.L. Banks, H.S. Beard, Y. Cao, A.E. Cho, W. Damm, R. Farid, A.K. Felts, T.A. Halgren, D.T. Mainz, J.R. Maple, R. Murphy, Integrated modeling program, applied chemical theory (IMPACT), J. Comput. Chem. 26 (2005) 1752-1780. https://doi.org/10.1002/jcc.20292.

[38] A.Y. Toukmaji, J.A. Board Jr, Ewald summation techniques in perspective: a survey, Comput. Phys. Commun. 95 (1996) 73-92. https://doi.org/10.1016/0010-4655(96)00016-1.

[39] J. Zielkiewicz, Structural properties of water: Comparison of the SPC, SPCE, TIP4P, and TIP5P models of water, J. Chem. Phys. 123 (2005) 104501. https://doi.org/10.1063/1.2018637.

[40] G.J. Martyna, M.L. Klein, M. Tuckerman, Nosé–Hoover chains: The canonical ensemble via continuous dynamics, J. Chem. Phys. 97 (1992) 2635-2643. https://doi.org/10.1063/1.463940.

[41] W.A. Powell, C.M. Catranis, C.A. Maynard, Design of self□processing antimicrobial peptides for plant protection, Lett. Appl. Microbiol. 31 (2000) 163-168. https://doi.org/10.1046/j.1365-2672.2000.00782.x.

Highlights

- Butanamides compounds were synthesized for the treatment of melanogenesis.
- In In-Vitro study we have performed Enzyme inhibition and kinetic analysis
- In-Vivo study also performed using Zebrafish model for melanogenesis
- In Computational study Molecular Docking and Simulation also performed
- Overall Compounds showed best results as compared to standard in all studies

Declaration of interests

☒ The authors declare that they have no known competing financial interests or personal relationships that could have appeared to influence the work reported in this paper.

☐The authors declare the following financial interests/personal relationships which may be considered as potential competing interests: